*Anal. Chem.* **2009,** *81,* 5474–5483

# Development of a Bioactive Paper Sensor for Detection of Neurotoxins Using Piezoelectric Inkjet Printing of Sol−Gel-Derived Bioinks

**S. M. Zakir Hossain,[†] Roger E. Luckham,[†] Anne Marie Smith,[†] Julie M. Lebert,[†] Lauren M. Davies,[‡] Robert H. Pelton,[‡] Carlos D. M. Filipe,[‡] and John D. Brennan*,[†]**

*Department of Chemistry, McMaster University, 1280 Main Street West, Hamilton, Ontario, L8S 4M1, Canada, and Department of Chemical Engineering, McMaster University, 1280 Main Street West, Hamilton, Ontario, L8S 4L7*

**There is an increasing interest in new strategies to rapidly detect analytes of clinical and environmental interest without the need for sophisticated instrumentation. As an example, the detection of acetylcholinesterase (AChE) inhibitors such as neurotoxins and organophosphates has implications for neuroscience, drug assessment, pharmaceutical development, and environmental monitoring. Functionalization of surfaces with multiple reagents, including enzymes and chromogenic reagents, is a critical component for the effective development of "dipstick" or lateral flow biosensors. Herein, we describe a novel paper-based solid-phase biosensor that utilizes piezoelectric inkjet printing of biocompatible, enzyme-doped, sol−gel-based inks to create colorimetric sensor strips. For this purpose, polyvinylamine (PVAm, which captures anionic agents) was first printed and then AChE was overprinted by sandwiching the enzyme within two layers of biocompatible sol−gel-derived silica on paper. AChE inhibitors, including paraoxon and aflatoxin B1, were detected successfully using this sensor by measuring the residual activity of AChE on paper, using Ellman's colorimetric assay, with capture of the 5-thio-2-nitrobenzoate ($TNB^-$) product on the PVAm layer. The assay provided good detection limits (paraoxon, ~100 nM; aflatoxin B1, ~30 nM) and rapid response times (<5 min). Detection could be achieved either by eye or using a digital camera and image analysis software, avoiding the need for expensive and sophisticated instrumentation. We demonstrate that the bioactive paper strip can be used either as a dipstick or a lateral flow-based biosensor. The use of sol−gel-based entrapment produced a sensor that retained enzyme activity and gave reproducible results after storage at 4 °C for at least 60 days, making the system suitable for storage and use in the field.**

Recently, paper-based patterned solid-phase sensors (which are simple, portable, disposable, and inexpensive) have been developed to run multiple bioassays and controls simultaneously.[1−7] These portable biosensing papers are extremely useful in remote settings and less-industrialized countries, where simple bioassays are essential in the first stages of detecting disease, and for monitoring environmental and food-based toxins. However, although these bioactive paper sensors show promise, all paper-based sensors reported to date have utilized biorecognition elements that are physically adsorbed onto the paper surface—no permanent immobilization method such as covalent or affinity attachment or entrapment techniques have been employed. As a result, paper-based sensors have been utilized only as lateral flow sensors and have not been amenable to dipstick sensing formats.

The automated deposition and permanent immobilization of biorecognition molecules on solid surfaces is a critical step in the development of bioactive paper-based sensors. To achieve this goal it is necessary to develop protein immobilization methods that are compatible with automated coating and/or printing methods and which retain the biomolecule at the surface of the paper substrate. In this work, we explore the use of biocompatible sol−gel-derived materials for this purpose. It has been shown that the entrapment of biomolecules within sol−gel-derived materials allows proteins to retain their bioactivity for prolonged periods of time.[8,9] Furthermore, sol−gel-based materials have previously been shown to be amenable to inkjet deposition (although not with proteins)[10] or screen printing with entrapped enzymes.[11] However, biocompatible sol−gel materials with entrapped proteins have not yet been deposited via inkjet printing and have not been incorporated within bioactive paper sensors.

* To whom correspondence should be addressed. Tel.: (905) 525-9140 (ext. 27033). Fax: (905) 527-9950. E-mail: brennanj@mcmaster.ca. URL: http://www.chemistry.mcmaster.ca/faculty/brennan.

[†] Department of Chemistry.

[‡] Department of Chemical Engineering.

(1) Li, X.; Tian, J.; Nguyen, T.; Shen, W. *Anal. Chem.* **2008**, *80* (23), 9131–9134.
(2) Abe, K.; Suzuki, K.; Citterio, D. *Anal. Chem.* **2008**, *80* (18), 6928–6934.
(3) Martinez, A. W.; Phillips, S. T.; Butte, M. J.; Whitesides, G. M. *Angew. Chem., Int. Ed.* **2007**, *46*, 1318–1320.
(4) Zhao, W.; Ali, M. M.; Aguirre, S. D.; Brook, M. A.; Li, Y. *Anal. Chem.* **2008**, *80* (22), 8431–8437.
(5) Bruzewicz, D. A.; Reches, M.; Whitesides, G. M. *Anal. Chem.* **2008**, *80* (9), 3387–3392.
(6) Su, S.; Ali, M. M.; Filipe, C. D. M.; Li, Y.; Pelton, R. *Biomacromolecules* **2008**, *9* (3), 935–941.
(7) Martinez, A. W.; Phillips, S. T.; Whitesides, G. M. *Proc. Natl. Acad. Sci. U.S.A.* **2008**, *105* (50), 19606–19611.
(8) Goring, G. L. G.; Brennan, J. D. *J. Mater. Chem.* **2002**, *12*, 3400–3406.
(9) Harrell, T. M.; Hosticka, B.; Power, M. E.; Cemke, L.; Hull, R.; Norris, P. M. *J. Sol−Gel Sci. Technol.* **2004**, *31*, 349–352.
(10) Di Risio, S.; Yan, N. *Macromol. Rapid Commun.* **2007**, *28* (18−19), 1934–1940.
(11) Wang, J.; Pamidi, P. V. A.; Park, D. S. *Anal. Chem.* **1996**, *68*, 2705–2708.



10.1021/ac900660p CCC: $40.75 
Published on Web 06/03/2009

Several conventional deposition techniques such as dip coating,[12] spin coating,[13] aerosol spraying, [14] and electrophoretic deposition[15] have previously been used to deposit bioactive sol−gel-derived materials. Among these, dip and spin coating are not practical for large-scale production. In addition, they are time-consuming and are wasteful when dealing with expensive bioreagents. Aerosol spraying can be used for the deposition of biomaterials, but the method is not easily adaptable to the formation of millimeter-scale patterns. Electrophoretic deposition is normally used for the fabrication of electrodes and the process requires an electrically conductive surface.[16]

On the other hand, the inkjet printing technique for deposition of materials on paper has attracted attention, because the system is simple, rapid, scalable, compatible with paper substrates, and amenable to pattern formation.[9,17−20] As a result, a variety of biomaterials can be deposited on a solid support in a single layer or multiple layers at ambient temperature with relatively low shear rates, with bioactivity being retained for extended periods.[21,22] Using this technology, cells/tissue,[23,24] DNA,[25] antibodies,[14] and enzymes[2,10,24] have been dispensed, deposited, or patterned in either two-dimensional (2D) or three-dimensional (3D) arrangements.

The most critical part of inkjet printing is probably the formulation of the bioink and its rheological properties, in particular, the viscosity and surface tension.[19,21] Several additives are introduced into ink formulations to optimize the physical properties and to make them stable and ejectable. The specific challenge associated with the formulation of enzyme-containing bioinks for reliable piezoelectric inkjet printing is retention of enzyme activity.[10] The printing of biocompatible sol−gel-derived inks is an even larger challenge, because the short gelation times of silica sols can cause gelation and clogging of the inkjet nozzles, especially when specific proteins (in buffer) are added to the sol−gel material. At physiological pH values, where most enzymes retain activity, gelation of most biocompatible sol−gel precursors occurs within a time frame of a minute to a few hours, depending on buffer strength and the type of additives being used.[26] For this reason, we have explored a multistage inkjet deposition method wherein the silica sol and the buffered protein are deposited from separate inkjet cartridges and, therefore, do not interact prior to deposition on the paper surface, avoiding gelation in the inkjet nozzle.

To evaluate the potential of inkjet deposition for fabrication of bioactive paper sensors, we have used the detection of organophosphates via inhibition of immobilized acetylcholinesterase (AChE) as a model system. Organophosphates (e.g., paraoxon) and mycotoxins (e.g., aflatoxin B1 (AfB1)) are classified as extremely hazardous compounds, because of their potent toxicity to the human nervous system.[27,28] Organophosphate compounds are widely used as agricultural pesticides, insecticides, and chemical warfare agents. These compounds are very stable and can rapidly diffuse into groundwater reservoirs and thus exhibit a threat of contamination. Mycotoxins—particularly, AfB1—are carcinogenic contaminants of food and animal feeds and, as such, are used as biochemical markers for food spoilage. The currently available methods for the determination of these compounds are liquid/gas chromatography,[29,30] optical and electrochemical biosensors,[31−34] surface plasmon resonance,[35] semiconductor quantum dots,[36] ion-selective field-effect transistors (ISFET),[37] and carbon nanotube[38] and nanoparticle-based sensors,[39,40] as well as several immunoassays.[35,41] Although these systems have high selectivity and adequate sensitivity, almost all of them either require sophisticated instrumentation, skilled operators, significant sample pretreatment, and/or long analysis times. Moreover, most of these detection systems are not amenable to rapid screening in emergency situations, in remote settings, or in developing countries, where simple and portable bioassays are essential for monitoring toxic compounds in the environment or foodstuffs. Therefore, it is critical to develop robust, highly sensitive, simple, stable, portable, and user-friendly methods to test for the presence of toxic compounds.

As a signal generation method, we have utilized the well-known Ellman colorimetric assay (see Scheme 1).[42] However, to allow permanent capture of the highly colored 5-thio-2-nitrobenzoate ($TNB^-$) anion, we have incorporated a cationic capture region onto the paper via inkjet printing of poly(vinylamine) (PVAm). The binding of toxins (e.g., paraoxon, AfB1) to AChE reduces


(12) Liu, J.; Mazumdar, D.; Lu, Y. *Angew. Chem., Int. Ed.* **2006**, *45*, 7955–7959.
(13) No, H.-Y.; Kim, Y. A.; Lee, Y. T.; Lee, H.-S. *Anal. Chim. Acta* **2007**, *594*, 37–43.
(14) Jordan, J. D.; Dunbar, R. A.; Bright, F. V. *Anal. Chem. Acta* **1996**, *332*, 83–91.
(15) Katagiri, K.; Hasegawa, K.; Matsuda, A.; Tatsumisago, M.; Minami, T. *J. Am. Ceram. Soc.* **1998**, *81* (9), 2501–2503.
(16) Van der Biest, O. O.; Vandeperre, L. T. *Annu. Rev. Mater. Sci.* **1999**, *29*, 327–352.
(17) Percin, G.; Khuri-Yakub, B. T. *Rev. Sci. Instrum.* **2003**, *74* (2), 1120–1127.
(18) Tsai, M. H.; Hwang, W. S.; Chou, H. H.; Hsieh, P. H. *Nanotechnology* **2008**, *19*, 335304–335313.
(19) Calvert, P. *Chem. Mater.* **2001**, *13* (10), 3299–3305.
(20) Allain, L. R.; Stratis-Cullum, D. N.; Vo-Dinh, T. *Anal. Chim. Acta* **2004**, *518*, 77–85.
(21) De Gans, B.-J.; Duineveld, P. C.; Schubert, U. S. *Adv. Mater.* **2004**, *16* (3), 203–213.
(22) Hasenbank, M. S.; Edwards, T.; Fu, E.; Garzon, R.; Kosar, T. F.; Look, M.; Mashadi-Hossein, A.; Yager, Y. *Anal. Chim. Acta* **2008**, *611*, 80–88.
(23) Xu, T.; Jin, J.; Gregory, C.; Hickman, J. J. *Biomaterials* **2005**, *26*, 93–99.
(24) Ilkhanizadeh, S.; Teixeira, A. I.; Hermanson, O. *Biomaterials* **2007**, *28*, 3936–3943.
(25) Bietsch, A.; Hegner, M.; Lang, H. P.; Gerber, C. *Langmuir* **2004**, *20*, 5119–5122.
(26) Besanger, T. R.; Hodgson, R. J.; Green, J. R. A.; Brennan, J. D. *Anal. Chim. Acta* **2006**, *564*, 106–115.
(27) Marrs, T. C. *Pharmacol. Ther.* **1993**, *58* (1), 51–66.
(28) Rosenfeld, C. A.; Sultatos, L. G. *Toxicol. Sci.* **2006**, *90* (2), 460–469.
(29) Blesa, J.; Seriano, J. M.; Molto, J. C.; Marin, R.; Manes, J. *J. Chromatogr. A* **2003**, *11*, 49–54.
(30) Ventura, M.; Gomez, A.; Anaya, I.; Diaz, J.; Broto, F.; Montserrat, A.; Luis, C. *J. Chromatogr.* **1990**, *1084*, 25–29.
(31) Arduini, F.; Errico, I.; Amine, A.; Micheli, L.; Palleschi, G.; Moscone, D. *Anal. Chem.* **2007**, *79*, 3409–3415.
(32) Harmon, H. J. *Biosens. Bioelectron.* **2001**, *16*, 1035–1041.
(33) Arduini, F.; Amine, A.; Moscone, D.; Ricci, F.; Palleschi, G. *Anal. Bioanal. Chem.* **2007**, *388*, 1049–1057.
(34) Goryacheva, Y.; De Saeger, S.; Eremin, S. A.; Petehhem, C. V. *Food Addit. Contam.* **2007**, *24* (10), 1169–1183.
(35) Lin, T.-J.; Huang, K.-T.; Liu, C.-Y. *Biosens. Bioelectron.* **2006**, *22*, 513–518.
(36) Gill, R.; Bahsahi, L.; Freeman, R.; Willner, I. *Angew. Chem.* **2008**, *120*, 1700–1703.
(37) Hai, A.; Ben-Haim, D.; Korbakov, N.; Cohen, A.; Shappir, J.; Oren, R.; Spira, M. E.; Yitzchaik, S. *Biosens. Bioelectron.* **2006**, *22*, 605–612.
(38) Liu, N.; Cai, X.; Lei, Y.; Zhang, Q.; Chan-Park, M. B.; Li, C.; Chen, W.; Mulchandani, A. *Electroanalysis* **2007**, *19* (5), 616–619.
(39) Pardo-Yissar, V.; Katz, E.; Wasserman, J.; Willner, I. *J. Am. Chem. Soc.* **2003**, *125*, 622–623.
(40) Pavlov, V.; Xiao, Y.; Willner, I. *Nano Lett.* **2005**, *5* (4), 649–653.
(41) Micheli, L.; Greco, R.; Badea, M.; Moscone, D.; Palleschi, G. *Biosens. Bioelectron.* **2005**, *21*, 588–596.
(42) Ellman, G. L.; Courtney, K. D.; Andres, V.; Featherstone, R. M. *Biochem. Pharmacol.* **1961**, *7*, 88–95.

**Scheme 1. Schematic Representation of the Detection Principle of the Ellman Assay[a]**

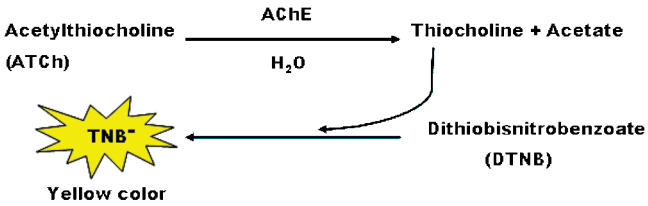


[a] Acetylcholinesterase (AChE) hydrolyzes the acetylethiocholine (ATCh) and forms thiocholine (TCh), which then reacts with dithiobisnitrobenzoate (DTNB) to generate 5-thio-2-nitrobenzoate (TNB, an anion), which is yellow in color.

AChE activity, and the residual activity is monitored based on the yellow color intensity that is produced. Following this simple and reliable assay mechanism, we show that it is possible to detect the AChE inhibitors in a rapid and cost-effective manner, using either a dipstick or lateral flow biosensing format.[31,43,44] This is the first report on the utilization of piezoelectric inkjet printing in the development of sol−gel-based paper biosensors; it provides a new platform for the fabrication of bioactive paper strips for the detection of drugs or environmental pollutants that affect both animals and humans.

## MATERIALS AND METHODS

**Chemicals.** Sodium silicate solution (~14% NaOH, ~27% $SiO_2$), tetraethylorthosilicate (TEOS, 98%), Dowex 50WX8-100 ion-exchange resin, acetylcholinesterase (AChE, from *Electrophorus electricus*, EC 3.1.1.7), paraoxon, aflatoxin B1 (AfB1, from *Aspergillus flavus*), 5,5′-dithiobis-(2-nitrobenzoic acid) (DTNB), carboxymethylcellulose sodium salt (CMC), and Triton X-100 were obtained from Sigma−Aldrich. Anhydrous glycerol and acetylthiocholine iodide (ATCh) were purchased from Fluka BioChemika Ultra (U.K.). Diglyceryl silane (DGS) was synthesized in our laboratory, using the transesterification of TEOS with anhydrous glycerol, as described in detail elsewhere.[45] PVAm (1.5 MDa) was obtained from BASF (Mississauga, Canada), as a gift. Mead brand cardboard paper substrate with a white hydrophobic clay coating (manufactured by Hilroy, Toronto, Canada) was purchased from the McMaster University Bookstore. Distilled deionized water ($ddH_2O$) was obtained from a Milli-Q Synthesis A10 water purification system (Millipore, Bedford, MA). All other reagents were of analytical grade.

**Procedures.** *Preparation of Solutions.* Stock solutions of the ATCh, paraoxon, and AfB1 were made daily and were not used for more than 3 h after preparation to minimize the potential for hydrolysis. Tris buffer (100 mM, pH 8) was used for the dilution of ATCh. A mixture of Tris buffer (50 mM, pH 6.8) and 5% cyclohexane (Sigma) was used for the dilution of paraoxon, whereas a mixture of Tris buffer (50 mM, pH 6.8) and 5% methanol (Sigma) was used for the dilution of AfB1. These solvents not only aid in dissolution of the AChE inhibitors, but also enhance the affinity of paraoxon[46] and aflatoxin[31] for binding to AChE. Furthermore, this level of organic solvent has been shown to have no effect on the stability of AChE. Note that experiments conducted without organic solvent present produced significantly lower detection limits for paraoxon or AfB1 (data not shown). Therefore, for practical applications, it is recommended that low levels of organic solvents be used, not only for dissolution purposes but also to enhance sensitivity. Distilled deionized water ($ddH_2O$) was used to dissolve PVAm. All other solutions were prepared using Tris buffer (100 mM, pH 8), if not otherwise stated. *CAUTION: Both AfB1 and paraoxon are extremely toxic. These materials should be handled with gloves and used in a fumehood.*

*Preparation of Sol−Gel Materials.* Two biocompatible sol−gel precursors—diglyceryl silane (DGS) and sodium silicate (SS)—were used to prepare sols for enzyme entrapment and printing onto paper. DGS sols were made by mixing 10 mL of $ddH_2O$ with 1 g of finely ground DGS. The mixture was sonicated in an ice bath for 20 min to dissolve the DGS and then filtered through a 0.22-$\mu$m membrane syringe filter to remove any particulates in the solution.

SS sols were prepared by mixing 10 mL of $ddH_2O$ with 2.9 g of sodium silicate solution (pH ~13), followed by the addition of 5 g of Dowex cation exchange resin to replace $Na^+$ with $H^+$. The mixture was stirred for 30 s to reach a final pH of ~4, and was then vacuum-filtered through a Büchner funnel. The filtrate was then further filtered through a 0.45-$\mu$m membrane syringe filter. These sols were used to formulate silica-containing inks, as described below.

*Construction of Bioactive Paper-Based Solid-Phase Sensor.* The papers were coated with a total of three different materials in a specific sequence. Generally, this involved (1) the printing of a PVAm underlayer directly onto the paper surface; (2) the printing of a silica sol intermediate layer; (3) the printing of a buffered enzyme solution that contained AChE (final concentration = 50 U/mL) and DTNB (final concentration = 500 $\mu$M); and (4) printing of a silica sol overlayer, as shown in Scheme 2. Between printing of the different silica and bio inks, 15−20 min was allowed for air drying. The different printing solutions (PVAm, sol or enzyme) were modified by the addition of glycerol, to control viscosity, and Triton X-100, to control surface tension, to optimize the printing performance (ability to jet the inks) as well as the enzyme activity, as described below. As noted in Table 1, the addition of glycerol to PVAm inks was not necessary, because the viscosity of an aqueous solution of this polymer was on the order of 3 cP. The high viscosity of the 0.5 wt % solution is likely due to the high molecular weight (ca. 1.5 MDa) of the polymer. The solutions were deposited using a piezoelectric inkjet printer (Model DMP-2800) from Fujifilm Dimatix, Inc. (Japan), using Drop Manager software (version 1.3.0.7). This system has a microelectromechanical system (MEMS)-based cartridge-style printhead that allows filling with desired bioinks (ca. 0.5−2 mL). Each cartridge has 16 nozzles linearly spaced at 254 $\mu$m with typical drop sizes of 1−10 pL. The instrument is equipped with a drop imaging system (Drop Watcher) that allows observation and capture of the events during drop formation on the printhead nozzles and the trajectory of the drops after ejection. Jetting conditions are described in Table 1. In all cases, the bioactive inks were printed by applying 16 piezo firings with one printing

(43) Marx, S.; Zaltsman, A. *Int. J. Environ. Anal. Chem.* **2003**, *83* (7−8), 671–680.
(44) Virel, A.; Laura, S.; Pavlov, V. *Anal. Chem.* **2009**, *81* (1), 268–272.
(45) Brook, M. A.; Chen, Y.; Guo, K.; Zhang, Z.; Brennan, J. D. *J. Mater. Chem.* **2004**, *14*, 1469–1479.
(46) Zhang, C.; Malhotra, S. V. *Talanta* **2005**, *67*, 560–563.

**Scheme 2. Schematic Illustration of Inkjet Printing Sequence of PVAm, Sodium Silicate (SS)-Based Sol−Gel-Derived Silica Matrix, and the Tris Buffer (100 mM, pH 8.0) Containing Enzyme Acetylcholinesterase (AChE) and Dithiobisnitrobenzoate (DTNB) Layers on Paper for the Development of a Portable Solid-Phase Biosensor**

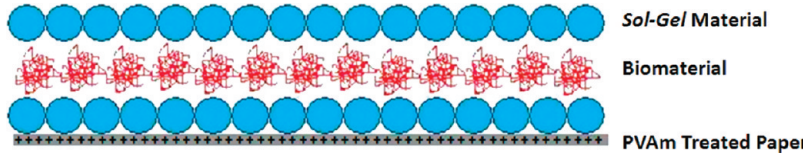


**Table 1. Bioink Formulations and Inkjet Deposition Parameters**

| Bioink Formulation (with 0.1 wt.% Triton X-100) | AChE Activity | Viscosity (cp) | Surface Tension (mN/m) | Jetting Conditions | Bioink Jettability | Movies of Drop Formation |
|---|---|---|---|---|---|---|
| **Bioinks for AChE** | | | | | | |
| Tris buffer (100mM, pH 8) | + | 1.01 ± 0.02 | 30~38 | Firing voltage: 40 v<br>Wave form: Single pulse. Fall in two steps<br>Pulse width: 70 µs<br>Meniscus vacuum : 4.0-4.5 inches $H_2O$<br>Firing frequency: 5 kHz | None | See supplementary movies |
| 1 % (v/v) Glycerol + Tris buffer | + | 1.06 ± 0.03 | | | None | |
| 10 % (v/v) Glycerol + Tris buffer | + | 1.35 ± 0.08 | | | Sporadic | |
| 20 % (v/v) Glycerol + Tris buffer | + | 1.91 ± 0.11 | | | Good | |
| 30 % (v/v) Glycerol + Tris buffer | + | 2.80 ± 0.13 | | | Excellent | |
| 40 % (v/v) Glycerol + Tris buffer | + | 4.21 ± 0.09 | | | Excellent | |
| 50 % (v/v) Glycerol + Tris buffer | + | 6.85 ± 0.21 | | | Excellent | |
| **Bioinks for SS *sol-gel* material** | | | | | | |
| Sodium silicate (SS) | + | 1.33 ± 0.04 | | | None | |
| 1 % (v/v) Glycerol + SS | + | 1.44 ± 0.07 | | | Poor | |
| 10 % (v/v) Glycerol + SS | + | 1.67 ± 0.10 | | | Sporadic | |
| 20 % (v/v) Glycerol + SS | + | 2.00 ± 0.13 | | | Good | |
| 30 % (v/v) Glycerol + SS | + | 2.67 ± 0.16 | | | Excellent | |
| 40 % (v/v) Glycerol + SS | + | 3.67 ± 0.19 | | | Excellent | |
| 50 % (v/v) Glycerol + SS | + | 6.00 ± 0.23 | | | Excellent | |
| **Bioink for PVAm** | | | | | | |
| PVAm (0.5 wt. %) | ** | 3.08 ± 0.14 | | | Excellent | |

[+] The AChE retains activity (>95%). ** Not applicable.

cycle per ink in a stepwise fashion in a 0.25 cm × 0.25 cm square pattern onto Mead brand cardboard (paper substrate, 10 cm × 8 cm), using a separate cartridge for each of the PVAm, silica, and enzyme "inks". For control experiments, a buffer that did not contain AChE was printed between the silica layers. Other controls involved printing of AChE + DTNB directly onto the PVAm underlayer without a silica coating, and printing of AChE + DTNB onto PVAm/silica without printing a silica overlayer.

*Ink Viscosity and Surface Tension Measurements.* The dynamic viscosity of the bioink components was measured using a capillary viscometer (Cannon−Fenske viscometer, size 75, Vineland, NJ) at room temperature. The viscometer was calibrated with Milli-Q water (viscosity ≈ 1 cP) before measuring the viscosity of the bioinks. Surface tension values were measured using a Krüss pendant drop apparatus. The shape of the pendant drop was analyzed using DSA10 shape analysis software by applying the Laplace equation. Pendant drops were formed by a Krüss needle with an outer diameter of 1.5 mm, which was connected to a 1-mL Perfektum glass syringe from Popper & Sons, Inc. Milli-Q water with a surface tension of 72.8 mN/m was used to calibrate the needle's inner diameter. All surface tension values of pendant drops were measured at 22 °C, with the temperature being controlled by a NESLAB thermostat system.

*Surface Topography.* Paper substrates were subjected to optical profilometry and scanning electron microscopy (SEM) imaging prior to deposition of any materials, after inkjet deposition of PVAm and after deposition of both PVAm and the silica/enzyme/silica layers. Optical profilometry images were obtained with a WYKO Model NT 1100 Optical Profiling System, using the VSI measurement mode and a magnification of 20×. For SEM analysis, samples were sputter-coated with platinum (layer thickness = 15 Å), to avoid charging effects, and were imaged using a JEOL, Ltd. (Tokyo, Japan) Model JSM-7000F instrument operating at 5 kV and a probe distance of 5.8 mm. The hydrophilic or hydrophobic nature of surface was also estimated by measuring the contact angle of dd$H_2O$ drop on paper using a Krüss pendant drop apparatus.

*Monitoring AChE Activity on Paper.* Prior to monitoring AChE activity on paper, the activity of AChE as a function of enzyme concentration was optimized. Different concentrations of AChE (0−200 U/mL) were entrapped in SS + 30% glycerol in a 96 well plate (total volume of 80 µL). A mixture (20 µL) of DTNB (500 µM) and ATCh (300 µM) was then added into each well and incubated for 5 min to allow color development. The absorbance at 412 nm was then measured using a TECAN Safire microwell plate reader.

The AChE activity on the bioactive paper strip was evaluated by measuring the color intensity produced by the enzymatic reaction using Ellman's method. The performance can be assessed in two ways: (a) by direct addition of substrate solution to the sensing area, or (b) by immersion of the paper strip into the substrate solution. The performance of the sensor was essentially the same for both of these cases. However, in the case of direct analyte addition, only small amounts of reagent were needed (5

μL), relative to dipstick sensors (~2 mL), reducing the cost per assay. For optimization of the AChE activity, small amounts (5 μL) of different concentrations of the substrate ATCh (0−500 μM) were added directly onto the sensing area of the paper strip and incubated for 5 min at room temperature to allow the yellow color to develop. The color intensity of the sensing areas was quantified by obtaining a digital image (Canon Model A630, 8.0 megapixels, operated in automatic mode with no flash and with the macroimaging setting on) and using ImageJ software to analyze the JPEG images. ImageJ software uses a 256-bit color scale, and, for our image processing, the images were inverted, so that areas that were originally white became black and corresponded to a color intensity of zero and areas that were originally black became white and corresponded to a color intensity of 256. Based on this scale, increases in the amount of yellow color cause an increase in color intensity of our sensor strips. To account for variations in color intensity that are due to differences in environmental illumination, a background subtraction (color intensity of the paper surface closest to the sensing area) was done for each data point.

The long-term stability of the enzyme printed on the paper strip was evaluated over a period of 60 days, with the paper strip stored at 4 °C. The assay conditions were the same as those described previously.

*Monitoring the Effect of PVAm.* To investigate the effect of the PVAm underlayer on the sensor performance, a lateral-flow-based paper chromatographic system was developed. In this case, strips of Whatman No. 1 filter paper (Sigma−Aldrich) were used in place of the Mead cardboard, because the Whatman paper is more hydrophilic and therefore supports the capillary flow of aqueous solutions. The Whatman paper strips (1 cm × 10 cm) were printed with aqueous inks that contained various levels of PVAm (0−1 wt %) and were allowed to air-dry for 15 min. The PVAm-treated strips were then immersed into a solution of 5-thio-2-nitrobenzoate ($TNB^-$, which is the colored product of the AChE-catalyzed reaction), which was produced enzymatically from ATCh (final concentration = 300 μM), DTNB (final concentration = 500 μM), and AChE (final concentration = 50 U/mL), with the sensing area above the liquid level. The retardation factor (Rf) was calculated based on the ratio of migration distance of the product ($TNB^-$), relative to the migration distance of solvent (Milli-Q water).

Lateral flow and dipstick assay formats were also developed to monitor the capability of PVAm to capture and preserve the color produced from the AChE-catalyzed reaction when performed on paper. In this case, Whatman (for lateral flow) or Mead cardboard dipsticks (1 cm × 10 cm) were prepared using inkjet-deposited PVAm (0 or 0.5 wt %), silica (SS + 30% glycerol) and AChE + DTNB (50 U/mL + 500 μM in 30% glycerol, with 1 wt % Triton X-100 present in all solutions) as described previously, followed by placing the sensor strip into a solution of substrate (300 μM ATCh) with the sensing area located above the liquid level (lateral flow) or within the solution (dipstick) and allowing the color to develop for 5 min. Following the assay, the resulting color intensity that remained on the paper strip was monitored once a day for up to three weeks.

*Measurement of AChE Inhibitors Using Bioactive Paper.* The inhibitory effects of paraoxon and AfB1 were evaluated using the solid-phase biosensor by measuring the decrease in the color intensity produced by the Ellman reaction. The PVAm/silica/AChE + DTNB/silica bioactive paper strip was first incubated with various concentrations of paraoxon solution (5 μL, 0−100 μM) or AfB1 solution (5 μL, 0−100 μM) for 10 min, after which point 10 μL of a solution of 300 μM ATCh was deposited onto the paper strip and incubated for 5 min. *[CAUTION: These assays should be performed in a fumehood using appropriate protective apparel.]* The intensity was determined by analyzing a digital image with ImageJ software, as described previously.

## RESULTS AND DISCUSSION

**Bioink Formulation and Jetting.** Initial attempts at inkjet deposition of sol−gel-based bioinks utilized silica sols to which buffered proteins had been added. While it was possible to produce protein-doped sols with relatively long gelation times, it was not possible to deposit such materials without gelation occurring in the nozzles of the inkjet cartridge. For this reason, all further studies on sol−gel-based inks utilized a multilayer deposition method, wherein the silica sol and buffered aqueous protein solutions were deposited from separate cartridges, to avoid mixing prior to deposition on the paper substrate.

Both the silica and aqueous protein "inks" were optimized to allow reproducible jetting onto paper substrates. Physicochemical properties such as surface tension and viscosity are critical parameters to make the ink stable and ejectable. Several additives (e.g., surfactants, viscosity modifiers) are generally incorporated in the ink formulations to optimize these rheological properties. However, inappropriate additives often may affect enzyme activity negatively. Therefore, it is essential to produce a suitable ink formulation in which the enzyme is active and, at the same time, produces stable and reproducible drops during jetting.

To adjust the ink surface tension (initially in the range of 60−78 mN/m without surfactant) to the printable range (30−40 mN/m), Triton X-100, which is a mild detergent, was used as a surfactant. To determine the effect of Triton X-100 on AChE activity, a solution of AChE (50 U/mL) in Tris buffer containing 0.1 wt % of Triton X-100 was prepared, and then the enzyme activity in solution was measured using the Ellman assay. No significant loss of AChE activity was observed in the presence of this low level of Triton X-100. Therefore, 0.1 wt % Triton X-100 was included in all bioink formulations (e.g., AChE, sol−gel-derived silica, PVAm) to get the optimum surface tension for printing (see Table 1).

To adjust the ink viscosity (initially in the range of 1.01−1.33 cP without viscosity modifiers) to the desired value (2−10 cP), two well-known viscosity modifiers—carboxymethylcellulose sodium salt (CMC) and anhydrous glycerol—were investigated. Polyethylene glycol (PEG) and poly(vinyl alcohol) (PVA), although biocompatible, were not examined, because these species have a tendency to promote macroscopic phase separation in sol−gel-derived silica,[47,48] which could result in significant protein leaching.[49] CMC, which is a charged polymer, was chosen because it has previously been demonstrated to be an effective viscosity

(47) Goring, G. L. G.; Brennan, J. D. *Chem. Mater.* **2007**, *19*, 5336–5346.
(48) Hodgson, R.; Chen, Y.; Zhang, Z.; Tleugabulova, D.; Long, H.; Zhao, X.; Organ, M. G.; Brook, M. A.; Brennan, J. D. *Anal. Chem.* **2004**, *76*, 2780–2790.
(49) Besanger, T. R.; Brennan, J. D. *J. Sol−Gel Sci. Technol.* **2006**, *40*, 209–225.

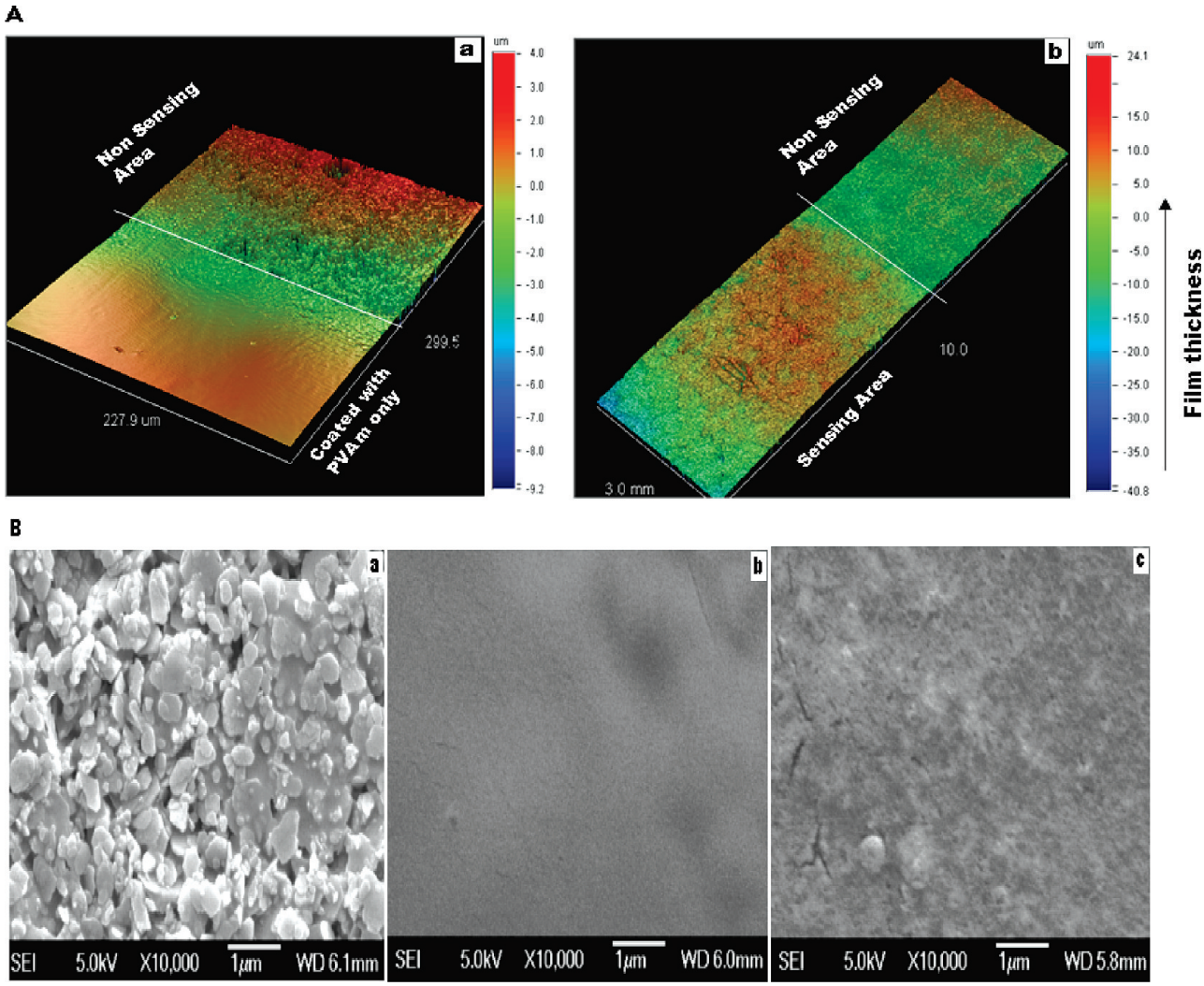


**Figure 1.** Topography of inkjet-sprayed PVAm, and AChE (50 U/mL) and DTNB (500 $\mu$M) doped sodium silicate (SS) thin films on paper. (A) Profilometry images of paper that is coated with or without PVAm only (panel a), and both PVAm and the silica/AChE + DTNB/silica layers (panel b). (B) SEM images of unmodified thin films (a), thin films modified with PVAm only (panel b), and thin films modified with PVAm, and AChE- and DTNB-doped silica on paper (panel c). The unmodified paper surface was rough, whereas the modified surfaces were relatively smooth.

modifier for inkjet deposition of horseradish peroxidase.[10] Glycerol was chosen because of its compatibility with both proteins[50] and with the sol−gel process.[45]

Initial studies on the effects of CMC (0−0.5 wt %) on AChE activity in solution showed that this additive led to a significant decrease in AChE activity at concentrations above 0.2 wt % (see Figure 1 in the Supporting Information). Therefore, CMC was not investigated further as a viscosity modifier. On the other hand, glycerol did not produce a decrease in AChE activity, even at levels of 30% v/v. The addition of this level of glycerol to either the SS-derived silica sol or AChE-based inks also resulted in excellent drop formation and jettability, as shown in Table 1. However, all inks prepared from DGS-derived silica sols, while jettable, resulted in poor adhesion and cracking after drying on the paper substrate and, therefore, were not investigated further. The origin of the cracking for DGS materials is not fully understood; however, the hydrolysis and condensation kinetics of DGS and sodium silicate are quite different, as has been noted in our previous papers.[51,52] This is likely to lead to a difference in the degree of cross-linking and significant differences in pore sizes. DGS has a larger proportion of small micropores, which are significantly affected by hydration stress during drying and rehydration.[45] This could explain the higher degree of cracking for DGS-based materials.

The drop formation and jettability of a series of silica-based inks are shown in movies that are available online as Supporting Information. Based on the excellent inkjetting properties and the high quality of the resulting deposited materials, all inks were formulated with 30% (v/v) glycerol and 0.1 wt % Triton-X100, using sodium silicate as the silica precursor.

**Coating Properties.** To characterize the coatings on paper substrates, optical profilometry, contact angles, and SEM images were obtained for both unmodified and modified paper substrates. Figure 1A shows optical profilometry images of paper that is

(50) Voss, R.; Brook, M. A.; Thompson, J.; Chen, Y.; Pelton, R. H.; Brennan, J. D. *J. Mater. Chem.* **2007**, *17*, 4854–4863.

(51) Tleugabulova, T.; Zhang, Z.; Brennan, J. D. *J. Phys. Chem. B* **2003**, *107*, 10127–10133.

(52) Tleugabulova, D.; Duft, A. M.; Zhang, Z.; Chen, Y.; Brook, M. A.; Brennan, J. D. *Langmuir* **2004**, *20*, 5924–5932.

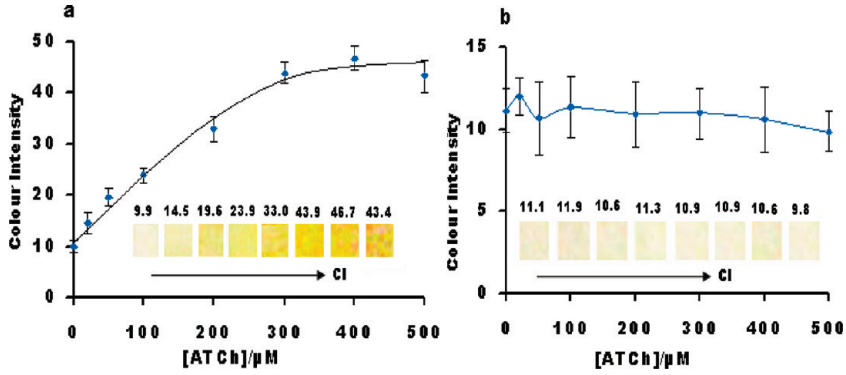


**Figure 2.** Dose-dependent effects of acetylthiocholine (ATCh) in the (a) presence and (b) absence of an AChE (50 U/mL)-doped silica matrix on paper, in which PVAm (0.5 wt %) was printed prior to printing of the silica and AChE layers. Inset is the color intensity (CI) generated at each ATCh concentration. All points are means (± the standard deviation) of five independent experiments for each concentration.

coated with PVAm only (panel a in Figure 1A), and with both PVAm and the silica/AChE + DTNB/silica layers (panel b in Figure 1A). No bioinks were printed on the non-sensing region. The profilometry results show that the PVAm layer is ~4 $\mu$m thick, whereas the sol−gel-based coating had an average thickness of ~24 $\mu$m. Similar results were obtained for layers printed on glass slides (data not shown), suggesting that the majority of the sensing layer was present on top of the paper, rather than within the paper. This is further supported by the contact angles for PVAm-coated and PVAm-free Mead cardboard and Whatman paper substrates, which were ~112.2 ± 1.1°, ~50.1 ± 0.3°, and 0°, respectively. The results indicate that the PVAm layer imparts high hydrophobicity to the paper surface, and, thus, liquid penetration into the surface is improbable.

Figure 1B shows SEM images of the unmodified paper (panel a in Figure 1B), PVAm-coated paper (panel b in Figure 1B), and paper that was coated with both PVAm and the silica/AChE + DTNB/silica layers (panel c in Figure 1B). The unmodified paper surface is very rough (average roughness of ±972 nm) and heterogeneous, and it clearly shows the presence of significant amounts of fillers (i.e., clay particles) at the surface of the paper and no evidence for paper fibers at the surface. This is consistent with the fact that the Mead paper used in this study had a protective coating. The deposition of PVAm resulted in a much smoother surface (±554 nm) and suggests that the cationic polymer likely provides a barrier coating above the filler layer onto which the silica layer is deposited, which is consistent with the data previously described. Thus, in addition to acting as an anion capture agent, PVAm also produces a more uniform surface, which may prevent enzyme leaching into the paper. Deposition of the silica/AChE + DTNB/silica layer resulted in a relatively homogeneous, crack-free layer (with a roughness of ±668 nm) that showed no evidence of large-scale macropores (those with a diameter of >0.5 $\mu$m), which is consistent with the inability of glycerol to act as a porogen. Taken together, the profilometry and SEM images show that the sol−gel-based ink layer is present on top of the paper, rather than penetrating through the paper. This is important, because it should help to retain the colorimetric signal within a thin layer, rather than having it diffuse throughout the thickness of the paper, making visualization easier.

**Monitoring AChE Activity and Its Storage Stability.** Prior to developing the dipstick sensor, the activity of AChE was evaluated as a function of enzyme concentration (0−200 U/mL) via the Ellman assay when entrapped in sol−gel-derived monolithic silica prepared from SS with 30% glycerol. The signal, which was measured 5 min after the addition of 300 $\mu$M ATCh and 500 $\mu$M DTNB, increased linearly over the concentration range from 0 U/mL to 50 U/mL, after which the signal showed negative deviation and reached a plateau at ~100 U/mL (data not shown). A value of 50 U/mL was chosen as the best compromise between a low enzyme loading, a sufficiently high signal (>4-fold increase over background) and good long-term stability. The high activity of entrapped AChE is in agreement with previous reports, showing that the enzyme is active and stable in sol−gel-derived silica materials.[53]

Based on the AChE activity data, a solid-phase bioactive paper-based sensor was constructed by multilayer inkjet printing of several bioinks in the following order: PVAm, silica, 50 U/mL AChE + 500 $\mu$M DTNB, and silica, using the compositions listed in Table 1, with 30% glycerol added to all inks except PVAm. This resulted in a layered system, as shown in Scheme 2. The effects of adding varying levels of ATCh over the bioactive paper sensor are shown in Figure 2a (a separate paper sensor is used for each ATCh concentration). Here, it is seen that, as the concentration of ATCh increases, the color intensity, recorded 5 min after the addition of the substrate over the sensing area, also increases. The color intensity saturated at a level of ~300 $\mu$M ATCh and suggested a $K_M$ value of ca. 150 $\mu$M, which is in good agreement with previous literature reports.[40] The color intensity was ~4-fold higher than that of a negative control (in the absence of ATCh but with AChE present).

To ascertain whether or not the supporting silica or PVAm materials degraded the DTNB or ATCh, a similar experiment was conducted using the same inks as those previously noted but with AChE absent from the aqueous ink layer. As shown in Figure 2b, the responses remained at the baseline signal upon the addition of varying levels of ATCh and were similar to signals obtained from control experiments performed in the absence of a substrate. Thus, our results confirm that the change in the color intensity is due to the AChE-catalyzed hydrolysis of ATCh to thiocholine iodide (TCh), which then reduces DTNB to $TNB^-$. Furthermore, this result shows that the AChE is able to withstand the shear forces associated with inkjet deposition and remains active when deposited between silica layers on a paper substrate.

(53) Pandey, P. C.; Upadhyay, S.; Pathak, H. C.; Panday, C. M. D.; Tiwari, I. *Sens. Actuators B* **2000**, *62*, 109–116.

The long-term stability AChE within the layered coating on the paper substrate was also investigated. Our results (shown in Figure 2 of the Supporting Information) demonstrated that the enzyme retained >95% of its initial activity over a period of at least two months when stored at 4 °C, indicating that both the enzyme and the DTNB reagent remained viable during storage. The observed stability of the enzyme, when entrapped in silica, is consistent with previous reports[51] and shows that the bioactive paper sensor should have a sufficient shelf life to allow storage and shipping.

To further assess the "sandwich architecture", two controls were performed to assess the effects of both the PVAm and the silica layers on AChE activity and stability. In the first case, the enzyme was printed directly onto PVAm without silica. In this case, the enzyme showed activity on day 1, but no activity by day 2, likely because of dehydration and/or strong electrostatic interactions between the enzyme and the cationic polymer, which caused denaturation. In the second case, the enzyme + DTNB solution was printed onto the silica material that covered the PVAm layer, but the silica overlayer was not added. Such sensors showed activity that was comparable to the "sandwich architecture" device after 2 days; however, after prolonged storage, the "non-sandwich" device produced significantly lower signal levels, as a result of enzyme inactivation. In addition, using this approach, it was not possible to use the sensor for dip-stick assays, because the enzyme readily desorbed from the sensor surface.

**Effects of PVAm on Biosensor Performance.** Two problems that were initially encountered when performing the Ellman assay using sol−gel-entrapped AChE on the paper-based sensor were (i) dispersion of the colored product over a large area, leading to lower color intensity, and (ii) the loss of color intensity with time. The former issue is expected, based on the ability of the low-molecular-weight colored product to readily move through the pores of the silica matrix and thus leach out of the sensing area. The latter issue seems to be related to a secondary chemical reaction of the $TNB^-$ with either the silica or some component in the paper, causing a complete loss of color intensity over a period of a few days (see below). This makes storage of used sensors for future reference impossible. Therefore, trapping and preserving the color within a finite region is required to obtain the highest output signals and keep the signal stable over long periods of time. We reasoned that the best method for capturing the anionic colored product was to introduce a cationic polymer (PVAm) onto the surface of the paper. This polymer has recently been shown to be useful for enhancing the wet strength of paper[54] and, therefore, should be compatible with the substrate, and it binds strongly to silica,[55] which should promote adhesion of the silica overlayer and not interfere with this coating layer. However, the introduction of PVAm directly to a silica sol causes very rapid gelation, because of base-catalyzed condensation; hence, this polymer was printed on paper prior to printing of the silica sol to avoid this problem.

To examine the effect of PVAm on sensor performance, a series of experiments were performed. Initial studies utilized a paper chromatographic setup (lateral flow-based) to assess the ability of PVAm coatings that contained varying levels of the polymer to retain the anionic product. For this purpose, hydrophilic Whatman No. 1 paper strips were printed with solutions that contained 0−1 wt % of PVAm and a solution of $TNB^-$ (produced by mixing 300 $\mu$M ATCh, 500 $\mu$M DTNB, and 50 U/mL of AChE in Milli-Q water) was allowed to travel up the paper via capillary action. Figure 3a shows values of the retardation factor (Rf), which is a measure of the relative mobility of $TNB^-$, as a function of PVAm concentration, and demonstrates that the Rf values decreased as the PVAm levels increased, up to a level of 0.5 wt % PVAm. Thus, 0.5 wt % PVAm was utilized in further studies to trap the negatively charged analyte.

Figure 3b shows the color intensity due to the elution of Ellman's solution using the lateral-flow-based paper chromatographic system. The areas within the dashed boxes were either treated or not treated (control) with 0.5 wt % PVAm that was deposited via inkjet spraying onto Whatman No. 1 paper, followed by printing of the silica/AChE + DTNB/silica layers over the same area. We found that PVAm was able to trap and concentrate the $TNB^-$ reaction product without diminishing the color intensity, while the unmodified paper (control) failed to trap the yellow color. As a result, the intensity of the yellow color was much higher when PVAm was present (in an area of 0.25 cm × 1 cm), which should produce a better detection limit when using the paper to sense an AChE substrate or inhibitors.

The capability of PVAm to preserve the $TNB^-$ product for an extended period of time was also investigated. For this, Mead cardboard dipsticks were coated with the PVAm ink, followed by silica/AChE + DTNB/silica ink layers and the dipsticks were immersed into a solution of 300 $\mu$M ATCh for 1 min. Images were obtained 30 min or 24 h after exposure to ATCh. A control sample was also tested in which the PVAm underlayer was not present. Figure 3c shows images of the dipsticks under the different testing conditions, and the figure clearly demonstrates that the PVAm is able to retain the yellow product while untreated paper causes the yellow color to disappear almost completely after only 24 h. Further testing revealed that the PVAm layer was capable of retaining the color for at least three weeks. Thus, the bioactive paper strips can be stored for future reference.

**Neurotoxin Measurement Based on AChE Inactivation.** Neurotoxins such as paraoxon and aflatoxin B1 are well-known inactivators of AChE.[27,28,31,46] The ability to detect these compounds using the inkjet-printed AChE-based paper sensor was investigated using an overspotting method, wherein small volumes of reagents were added directly to the sensing area. In this case, as little as 10 $\mu$L of solutions that contain various concentrations of paraoxon or AfB1 could be tested by applying them onto the sensing area of the strip, incubating for 10 min at room temperature, adding 10 $\mu$L of a solution containing 300 $\mu$M ATCh, and finally measuring the color intensity after 5 min using a digital camera and image processing software. Figure 4a shows the dose-dependent inhibition effects of paraoxon, while Figure 4b shows the semilogarithmic plot of color intensity, corresponding to the same experiments, demonstrating an $IC_{50}$ value in the range of 1 $\mu$M and a detection limit (S/N = 3) of ca. 100 nM. Figures 5a and 5b show the dose-dependent inhibition responses and a semilogarithmic plot of color intensity, respectively, for AfB1, and show that the $IC_{50}$

(54) Koruso, K.; Pelton, R. *J. Pulp Paper Sci.* **2004**, *30*, 228–232.
(55) Sharma, J.; Tleugabulova, D.; Czardybon, W.; Brennan, J. D. *J. Am. Chem. Soc.* **2006**, *128*, 5496–5505.

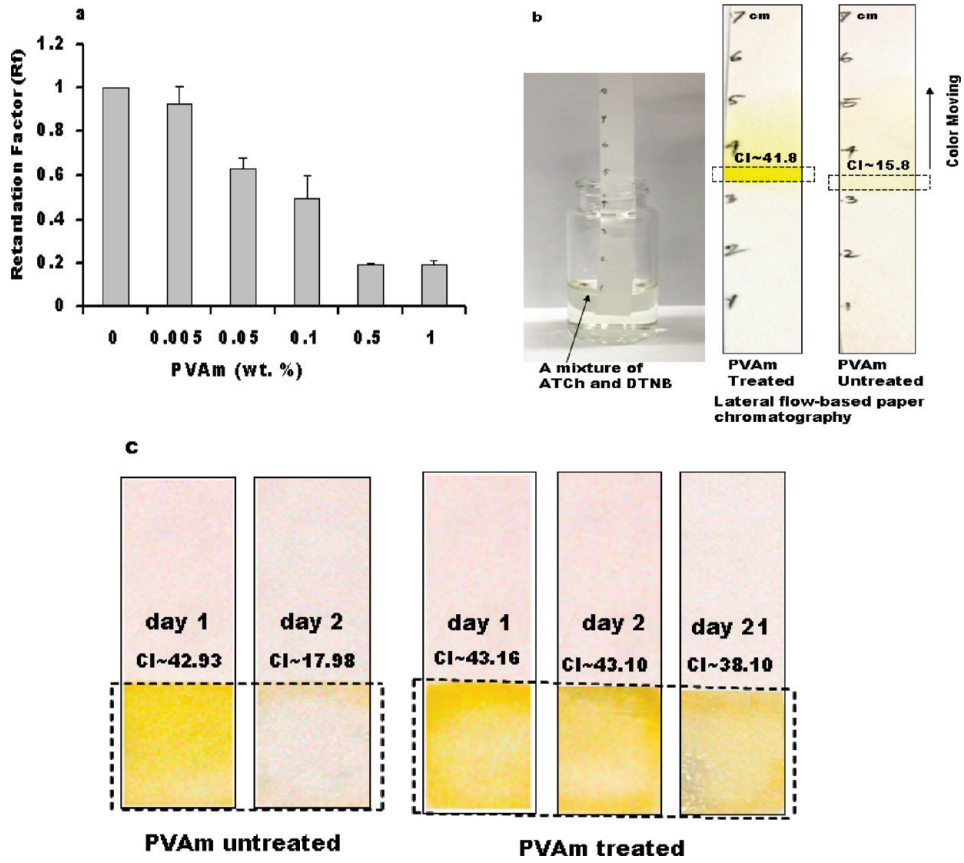


**Figure 3.** Effects of cationic PVAm on entrapment, as well as preservation of the anionic TNB in a lateral-flow-based paper chromatographic system: (a) The values of retardation factor (Rf) for anionic TNB in Milli-Q water in the presence of indicated PVAm levels. (b) Color intensity (CI) due to elution of ATCh (300 $\mu$M, final concentration) in the lateral-flow-based platform. The areas within the dashed boxes were printed without (control) and with PVAm (0.5 wt %), followed by the printing of AChE (50 U/mL). PVAm concentrates the reaction product (the yellow TNB anion), while in the control experiment, the yellow TNB anion is dispersed over a large area. (c) Cardboard dipstick with inkjet-printed PVAm or control (no PVam) and silica/AChE/DTNB/silica layers after being immersed in a ATCh solution. Both materials show an initial color response, but only the PVAm (0.5 wt %)-treated paper retains the reaction product (a yellow $TNB^{-}$) for a period of 3 weeks, whereas the PVAm-untreated paper failed to retain the color.

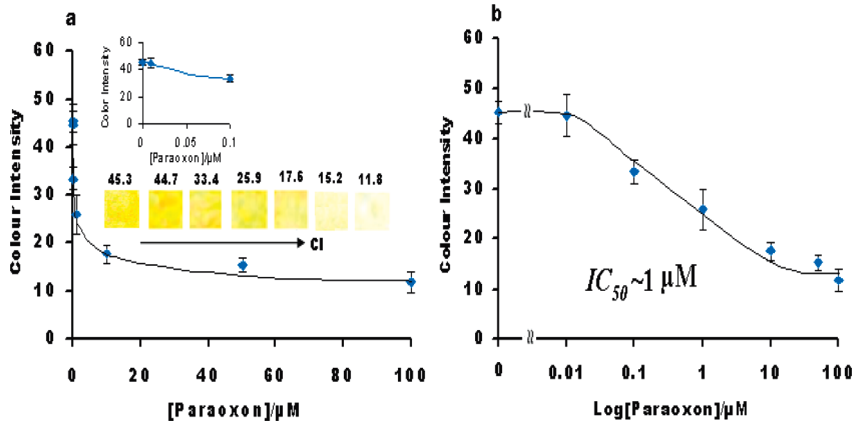


**Figure 4.** (a) Dose-dependent inhibition of acetylcholinesterase (AChE) by various concentrations of paraoxon. Insets are the color intensity (CI) at each paraoxon concentration and dose-dependent inhibition responses with the lower levels of paraoxon. (b) Semilogarithmic plot of the data in panel a. PVAm and AChE (50 U/mL)-and DTNB-doped silica layers were printed on paper before the experiments were conducted. All points are means ($\pm$ the standard deviation) of five measurements for each concentration.

value in this case is ca. 100 nM, with a limit of detection (LOD) of ~30 nM. A comparison of the responses obtained at 100 nM of either paraoxon or AfB1 show that AfB1 is a more potent inhibitor (~45% inhibition vs ~25% inhibition for paraoxon), which is consistent with previous studies.[31,35,40]

The insets for Figures 4 and 5 show the images of the paper strips at each inhibitor concentration, and the data clearly demonstrate that detection of the inhibitors is possible using the naked eye. This is an important aspect of the bioactive paper strips, because this permits the use of the test strips directly in the field

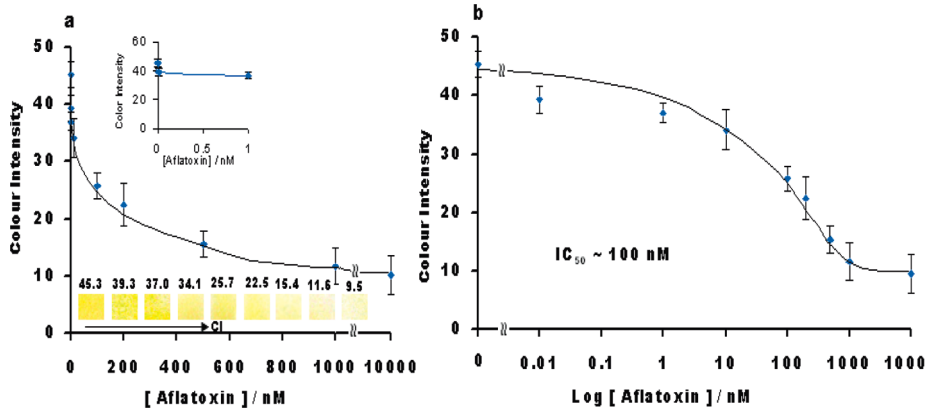


**Figure 5.** (a) Dose-dependent inhibition effects of aflatoxin B1 (AfB1) on AChE activity. Insets are the color intensity (CI) at each AfB1 concentration and dose-dependent inhibition responses with the lower levels of AfB1. (b) Semilogarithmic plot of the data shown in panel a. Data are means (± the standard deviation) of five independent measurements for each concentration.

and eliminates the need for sophisticated instrumentation. The presence of a simple colorimetric readout also enables rapid imaging and transmission to a central laboratory for further quantitative analysis using a simple cell phone camera combined with e-mail or MMS messaging.[3,5,7] Hence, rapid, on-site qualitative or quantitative analysis of organophosphates or aflatoxins should be possible using this bioactive paper platform.

## CONCLUSION

In this study, we introduced a novel sol−gel-based method for coating enzymes onto paper substrates using inkjet printing of various "ink" layers to produce a bioactive paper sensor for the detection of acetylcholinesterase (AChE) substrates and inhibitors, based on Ellman's colorimetric assay. Our data show that AChE can be printed between two biocompatible silica layers on paper and that the enzyme retains full activity for at least 2 months when stored at 4 °C. The use of PVAm as a cationic capture agent on the paper significantly enhances the signal intensity, because of its ability to concentrate the anionic $TNB^-$ product in a finite region, and it also retains the signal over several months. When used in combination with digital imaging and image processing, the bioactive paper sensor can be used for the quantitative assessment of AChE inhibitors, including paraoxon and aflatoxin B1 (AfB1), by monitoring the residual activity of the entrapped enzyme. Our experimental data are consistent with those previously reported using conventional instrumental methods. The ability to utilize inkjet printing for the deposition of biological reagents opens the door to the automated fabrication of bioactive paper sensors, and it should enable elaborate patterns of enzymes to be printed to produce multianalyte sensor strips. The entrapment of the enzyme at the paper surface allows the sensor to be used for either lateral flow or dipstick sensing applications, and it eliminates the potential for enzyme leaching. A drawback of the current sensor is the need to have the substrate, acetylthiocholine iodide (ATCh), present in the test solution, making it necessary to perform a sample pretreatment step prior to analysis. Further efforts are needed to modify this bioactive solid-phase paper sensor into a fully reagentless, multiplexed, and small-sample-volume biosensor. Our efforts in these areas will be reported in future work.

## ACKNOWLEDGMENT

The authors thank the Natural Sciences and Engineering Research Council of Canada (NSERC) for funding this work through a network grant−SENTINEL Canadian Network for the Development and Use of Bioactive Paper. The authors also thank the Canada Foundation for Innovation and the Ontario Innovation Trust for support of this work. J.M.L. thanks NSERC for providing a Canada Graduate Scholarship. R.H.P. holds the Canada Research Chair in Interfacial Technologies. J.D.B. holds the Canada Research Chair in Bioanalytical Chemistry.

## SUPPORTING INFORMATION AVAILABLE

Supporting Information is available as noted in the text. (PDF, AVI) This material is available free of charge via the Internet at http://pubs.acs.org.free of charge.

Received for review March 30, 2009. Accepted May 5, 2009.

AC900660P